BMC Biology

RESEARCH

Open Access

Cyclic stretch enhances neutrophil extracellular trap formation

Manijeh Khanmohammadi[1,2], Habiba Danish[1,2], Nadia Chandra Sekar[1,2], Sergio Aguilera Suarez[3], Chanly Chheang[2], Karlheinz Peter[1,2,4], Khashayar Khoshmanesh[2,3] and Sara Baratchi[1,2,4*]

Abstract

Background Neutrophils, the most abundant leukocytes circulating in blood, contribute to host defense and play a significant role in chronic inflammatory disorders. They can release their DNA in the form of extracellular traps (NETs), which serve as scaffolds for capturing bacteria and various blood cells. However, uncontrolled formation of NETs (NETosis) can lead to excessive activation of coagulation pathways and thrombosis. Once neutrophils are migrated to infected or injured tissues, they become exposed to mechanical forces from their surrounding environment. However, the impact of transient changes in tissue mechanics due to the natural process of aging, infection, tissue injury, and cancer on neutrophils remains unknown. To address this gap, we explored the interactive effects of changes in substrate stiffness and cyclic stretch on NETosis. Primary neutrophils were cultured on a silicon-based substrate with stiffness levels of 30 and 300 kPa for at least 3 h under static conditions or cyclic stretch levels of 5% and 10%, mirroring the biomechanics of aged and young arteries.

Results Using this approach, we found that neutrophils are sensitive to cyclic stretch and that increases in stretch intensity and substrate stiffness enhance nuclei decondensation and histone H3 citrullination (CitH3). In addition, stretch intensity and substrate stiffness promote the response of neutrophils to the NET-inducing agents phorbol 12-myristate 13-acetate (PMA), adenosine triphosphate (ATP), and lipopolysaccharides (LPS). Stretch-induced activation of neutrophils was dependent on calpain activity, the phosphatidylinositol 3-kinase (PI3K)/focal adhesion kinase (FAK) signalling and actin polymerization.

Conclusions In summary, these results demonstrate that the mechanical forces originating from the surrounding tissue influence NETosis, an important neutrophil function, and thus identify a potential novel therapeutic target.

Keywords Cyclic stretch, Mechanotransduction, Substrate stiffness, Neutrophils, NETosis

Background

Neutrophils are characterized by their multilobed nucleus and are central as the first line of defense against bacterial infection [1, 2]. They migrate toward the site of infection within minutes following trauma and respond to pathogens via phagocytosis [3]. Moreover, neutrophil recruitment to the site of inflammation is triggered by releasing signaling molecules and chemokines [4, 5]. Neutrophils can release their DNA in the form of extracellular traps, called NETs, which serve as a scaffold for capturing various blood cells, bacteria, and other pathogens [6–8]. The formation of NETs, which is termed

*Correspondence:
Sara Baratchi
sara.baratchi@baker.edu.au
[1] School of Health and Biomedical Sciences, RMIT University, Melbourne, VIC, Australia
[2] Baker Heart and Diabetes Institute, Melbourne, VIC, Australia
[3] School of Engineering, RMIT University, Melbourne, VIC, Australia
[4] Department of Cardiometabolic Health, The University of Melbourne, Melbourne, VIC, Australia

NETosis, is initiated by chromatin decondensation, ruptured nuclear envelope and plasma membrane, and consequent extrusion of NETs to the extracellular space [6, 9, 10]. Although neutrophil activation and NETosis are critical for the innate arm of the immune system, the surrounding tissue can be damaged during uncontrolled NETosis [11–13]. Excess NETosis can lead to excessive activation of coagulation pathways and thrombosis, contributing to the pathogenesis of autoimmune and cardiovascular diseases (CVDs) [14].

Neutrophils in circulation are constantly exposed to hemodynamic forces, which affect their basic biology, including their ability to form NETs within sterile thrombi and the expression of inflammatory chemokines and cytokines [15, 16]. In addition to hemodynamic forces, once migrated into the tissue, these cells experience mechanical forces from their surrounding environment and the impact of transient changes in tissue mechanics that occur with the natural aging process, infection, tissue injury, and cancer on neutrophils remains unknown.

Cyclic stretch is the repetitive mechanical deformation of the artery walls as they lengthen to accommodate increased blood pressure during systole and return to their normal state due to their elastic properties during diastole [17]. Physiologic levels of cyclic stretch within the range of 6–12% are needed for mediating endothelial cell functions in arteries [18, 19], vascular smooth muscle cell contractile phenotype and controlling gene expression of extracellular matrix components [20] as well as synthesis and secretion of various macromolecules [21] by endothelial cells and vascular smooth muscle cells. In contrast, a high level of cyclic stretch (20%) due to hypertension or low level of cyclic stretch (<3%) due to aging causes cell apoptosis [21–26].

The influence of cyclic stretch on the various cell types within the different layers of the human blood vessel wall, including vascular smooth muscle cells [27–29], fibroblasts [30, 31], and endothelial cells [26, 32, 33], has been widely investigated via flow-free cell stretch systems. Immune cells, such as neutrophils that adhere to the vessel wall, are also exposed to stretch due to cyclic deformation of the vessel wall resulting from cardiac contractile function. However, the role of neutrophils and the molecular mechanisms that control NETosis under cyclic stretch has been largely unknown.

On the other hand, vascular aging is related to the loss of arterial elasticity, known as arterial stiffness, due to the degeneration of the arterial elastic fibers and collagen deposition at the vessel wall [34]. These vascular changes can be influenced by hemodynamic forces such as cyclic stretch [35, 36] and factors such as hormones, cytokines, salt, and glucose levels [37]. Studies have determined that neutrophil activation and release of NETs are also more widespread in aged arteries [38]. PAD4 is a calcium-dependent enzyme that citrullinates histones during neutrophil activation [39, 40]. A comparison between aged PAD4−/− mice and aged wild-type mice revealed that collagen deposition, along with disruption in systolic and diastolic function leading to NETosis, was present only in wild-type mice, suggesting a role for PAD4 in age-related organ dysfunction [38]. Clinical studies have shown that arterial stiffness in aged individuals is considered an independent risk factor for CVDs [41, 42]. Interestingly, it has been demonstrated that the phenotype and functionality of macrophages [43, 44] and dendritic cells [45] are affected by alterations in matrix elasticity. Furthermore, tissue stiffness as seen in disorders such as atherosclerosis [46], organ fibrosis [47], and cancer [48] may lead to the release of pro-inflammatory markers and even more tissue stiffness [38]. Several studies have reported that matrix elasticity changes affect neutrophils' adhesion, migration, and chemotaxis [49–51]. Furthermore, it has been shown that the activation of β2 integrins is important for neutrophil adhesion, migration, and NETosis [52, 53]. The integrin/focal adhesion kinase (FAK) signaling pathway has an important role in stiffness-dependent NETosis [16]. Additionally, neutrophil migration through the endothelium is regulated by matrix elasticity [54]. In humans, numerous studies have elucidated the contribution of integrin signaling to NETosis, although the respective findings are partially inconsistent [55, 56]. It has been suggested that LPS-mediated NETosis depends on the elasticity/stiffness of surrounding tissues [11].

However, the impact of substrate stiffness in conjunction with adhesion-related processes on NETosis is not fully understood and remains an open question. This work evaluates the potential impact of substrate stiffness and cyclic stretch on NETosis and identifies the downstream signaling pathway activated post cyclic stretch stimulation.

Results

Synergic cyclic stretch and substrate stiffness induces chromatin decondensation in neutrophils

To assess the synergic effect of substrate stiffness and cyclic stretch on NETosis, we cultured neutrophils inside elastomeric wells with defined stiffness levels of 30 and 300 kPa. These values were selected based on previous human studies showing that in young adults, the stiffness of the ascending aorta is within the range of 20–30 kPa, while by the age 80, the average elastic moduli increase to 200–300 kPa [57] (Fig. 1A).

The wells were pre-coated with collagen 1 to facilitate the adhesion of cells. Following cyclic stretch stimulation,

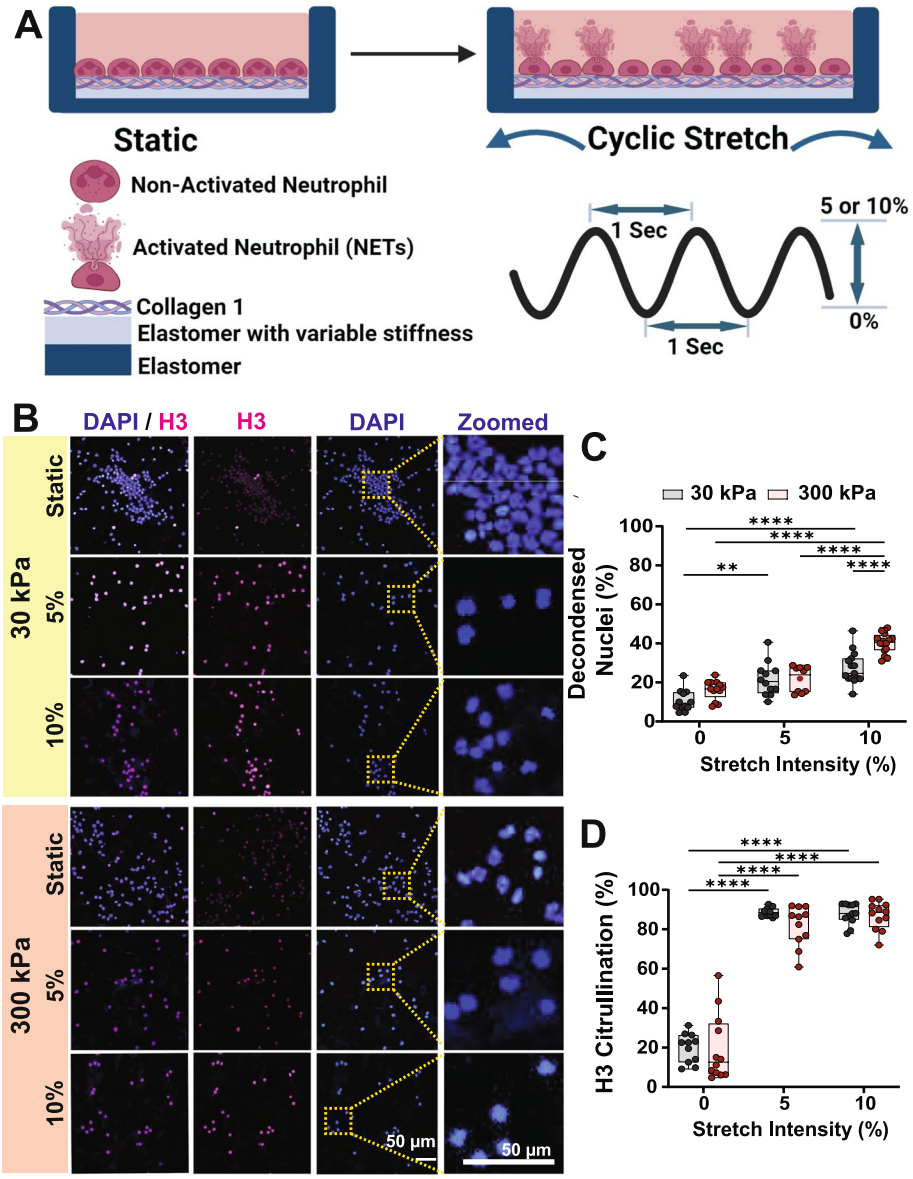

Fig. 1 Substrate stiffness and cyclic stretch modulate NETosis. **A** Schematic cartoon, showing different experimental conditions used in this study (figure created with BioRender.com). **B** Representative immunofluorescence images of human neutrophils stained with DAPI and CitH3 antibody under control or cyclic stretch. **C** Percentage of neutrophils with decondensed nuclei. **D** Percentage of cells stained positive for CitH3 after exposure to 5% and 10% cyclic stretch in the presence of two substrates with stiffness levels of 30 and 300 kPa. Boxes show the median and first and third quartiles. Whiskers represent minimum to maximum values. Bar graphs are representative of at least 3 independent experiments, and each dot represents a randomly selected field of view with at least 3 images analyzed per experiment. Statistical significance was determined using two-way ANOVA and multiple comparison tests. $^{**}P < 0.01$ and $^{****}P < 0.0001$

the degree of chromatin decondensation and NETs production was assessed using DAPI staining.

Overall, increase of stretch intensity improved the percentage of neutrophils with decondensed nuclei without any detectable NETs. For example, using the stiff substrate, applying cyclic stretch of 5% and 10% led to 2.3 ± 1.3-fold and 3 ± 1.15-fold ($P < 0.0001$) increase in the percentage of the decondensed nuclei compared to static conditions, respectively (Fig. 1B, C). In addition, we found that increasing the substrate stiffness from 30 to 300 kPa under a 10% cyclic stretch led to a 1.6 ± 0.46-fold ($P < 0.0001$) increases in the percentage of the decondensed nuclei (Fig. 1B, C). However, for neutrophils cultured under static or 5% cyclic stretch, increase of substrate stiffness did not affect the degree of nuclear decondensation.

Next, we assessed the effect of cyclic stretch on the citrullination of histone H3 (CitH3), which is widely used as marker for NETs formation both in vivo and in vitro studies [58]. Consistent with the percentage of cells with decondensed nuclei, applying cyclic stretch of 5% and 10% increased the percentage of cells with positive H3 staining, compared to static conditions, regardless of substrate stiffness (Fig. 1B–D). These results suggested that cyclic stretch can directly induce NETosis in a stretch dependent manner.

Cyclic stretch and substrate stiffness improve the sensitivity of neutrophils to PMA, LPS, and ATP

Next, we assessed the combined effect of cyclic stretch and substrate stiffness on the sensitivity of neutrophils to NET-inducing agents. For this, we used the most commonly used NET inducing agents, including phorbol myristate acetate (PMA), lipopolysaccharide (LPS), and adenosine triphosphate (ATP) [59].

Neutrophils were exposed to cyclic stretch and substrate stiffness in the presence or absence of 75 nM PMA, 10 μg/mL LPS, or 100 nM ATP. Based on our preliminary assessments, these concentrations, in the absence of cyclic stretch, led to moderate NETosis. Initially, we assessed the direct effect of these stimuli in the absence of stretch on NETosis. As expected, we found that these concentrations significantly increased NETosis in the absence of cyclic stretch; however, changes in substrate stiffness did not affect the sensitivity of neutrophils to these NET-inducing agents (Supplementary Fig. 1). As expected, under static conditions, all three agents induced NETosis; however, by assessing the NET area, we found that an increase in cyclic stretch and substrate stiffness improved the sensitivity of neutrophils to all three agents (Fig. 2A–D). For example, for neutrophils cultured on a stiff substrate, increase of cyclic stretch from 5 to 10% led to a 1.3 ± 0.5-fold ($P < 0.05$) increase in NETs area in the presence of ATP (Fig. 2G). Under

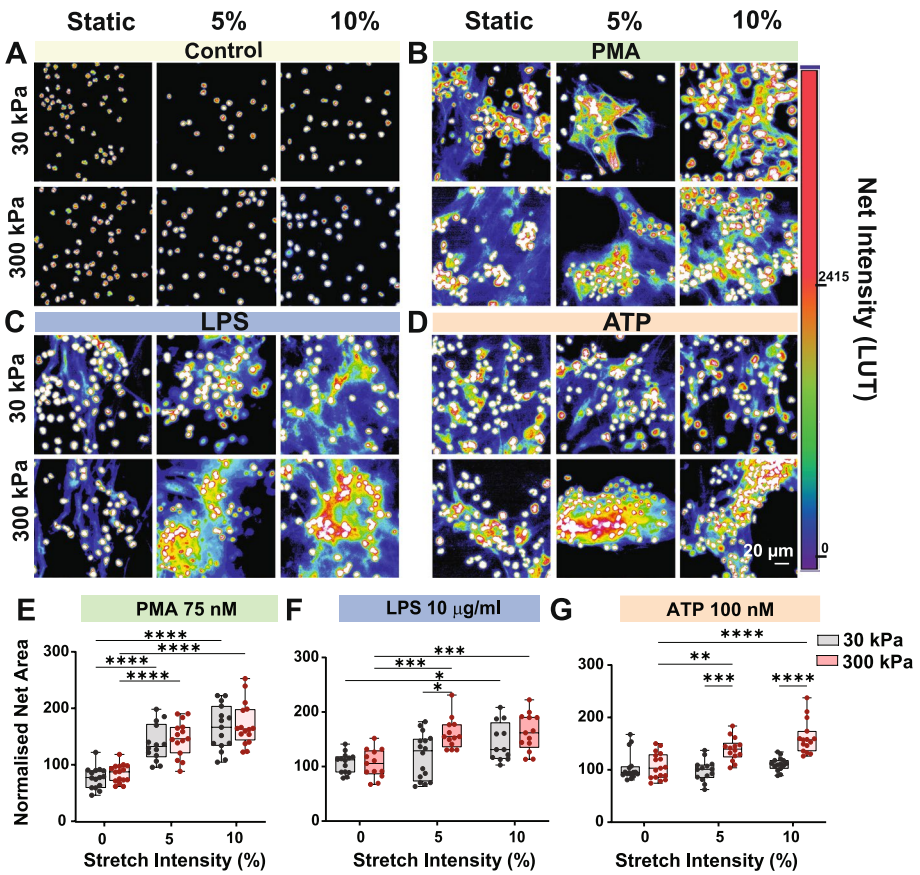

Fig. 2 Cyclic stretch increased the sensitivity of neutrophils to NETs-inducing agents. **A**–**D** Representative immunofluorescence images and **E**–**G** Bar graphs showing NETs areas normalized to total cell number after exposure to 5% and 10% cyclic stretch or static condition in the presence or absence of PMA (75 nM), LPS (10 μg/mL), or ATP (100 nM). Boxes show the median and first and third quartiles. Whiskers represent minimum to maximum values. Bar graphs are representative of at least 4 independent experiments, and each dot represents a randomly selected field of view, with at least 3 images per experiment. Statistical significance was calculated using two-way ANOVA and multiple comparison tests. *$P < 0.05$, **$P < 0.01$, ***$P < 0.001$, and ****$P < 0.0001$

static conditions, increasing the substrate stiffness did not affect NETs area. In comparison, under cyclic stretch increasing the substrate stiffness affect the NETs production. For example, increase of substrate stiffness from 30 to 300 kPa under 5% cyclic stretch led to 1.54 ± 0.62-fold ($P < 0.05$) and 1.48 ± 0.5-fold ($P < 0.01$) increase in NETs area in response to LPS and ATP, respectively (Fig. 2F, G). However, changing the substrate stiffnesses did not significantly increase the NETs area in response to PMA, most likely because the response was already saturated (Fig. 2E).

Cyclic stretch-induced NETosis is regulated via cytoskeleton remodeling and the PI3K/AKT signaling pathway

Given that the PI3K/AKT/integrin-mediated signaling pathway has been linked to several vascular responses to hemodynamic forces [60], we aimed to assess the contribution of PI3K/AKT signaling in neutrophil responses to cyclic stretch and substrate stiffness. Hence, human neutrophils were pretreated by PF573228, which is an inhibitor of FAK, or LY294002, which is an inhibitor of PI3K, followed by exposure to cyclic stretch in the presence of a stiff substrate (Fig. 3A). Using this approach, we found that inhibition of FAK or PI3K leads to 3.1 ± 0.65-fold ($P < 0.0001$) or 4 ± 1.40-fold ($P < 0.0001$) reduction in the percentage of the decondensed nuclei, and 3.1 ± 0.72-fold ($P < 0.0001$) or 3.2 ± 0.93-fold ($P < 0.0001$) reduction in the percentage of cells with positive H3 staining, compared to the vehicle control group (Fig. 3B, C).

To confirm the effect of cyclic stretch and substrate stiffness on the activation of the PI3K signaling pathway, we assessed AKT activity in response to cyclic stretch with or without LY294002, a PI3K inhibitor upstream of AKT. Subsequently, AKT activation was assessed by measuring the percentage of cells stained positive for phospho-AKT. Using this approach, we observed a 2.2 ± 1.2-fold increase ($P < 0.0001$) in the percentage of neutrophils stained positive for phospho-AKT in response to cyclic stretch compared to the static control (Fig. 3D, E). Additionally, pretreatment of cells with LY294002 resulted in a 6.9 ± 2.2-fold reduction ($P < 0.0001$) in the percentage of phospho-AKT-positive cells compared to the cyclic stretch group (Fig. 3D, E).

Next, we assessed the contribution of cytoskeleton remodeling by inhibiting the MLCK activity using ML-7 or actin polymerization using latrunculin A (Fig. 4A). Using this approach, we found that pretreatment of cells with ML-7 and latrunculin A inhibitors leads to 3.3 ± 0.83-fold ($P < 0.0001$) and 4.25 ± 2.01-fold ($P < 0.001$) decrease in the percentage of decondensed nuclei and 5.1 ± 1.4-fold ($P < 0.0001$) or 4.4 ± 1.4-fold ($P < 0.0001$) reduction in the percentage of cells with positive H3 staining, respectively (Fig. 4B, C). To confirm the effect of cyclic stretch and substrate stiffness on cytoskeleton remodeling, we assessed the impact of cyclic stretch on the intensity of polymerized versus monomeric actin using F and G-actin staining. Through this approach, we observed that an increase in stretch intensity from zero to 10% resulted in a 1.8 ± 0.5-fold ($P < 0.001$) increase in the F/G-actin ratio. Overall, this experiment confirms that cyclic stretch enhances cytoskeleton remodeling in neutrophils (Fig. 4D, E).

Calpain activity control neutrophils responses to cyclic stretch

Given that Calpain activity via Ca^{2+} influx is the key step for neutrophil flattening morphology transition and NETosis [61], we aimed to assess the contribution of calcium-activated protease, Calpain, in stretch-induced NETosis. Initially, we used a Calpain activity assay that utilizes a synthetic fluorogenic substrate to monitor total levels of Calpain activity in neutrophils post exposure to cyclic stretch. Using this approach, we found that stimulation of neutrophils with 10% cyclic stretch for 3 h increases the Calpain activity by 1.4 ± 0.14-fold ($P < 0.0001$) compared to the static group (Fig. 5A).

Next, we pre-treated the neutrophils with two classes of Calpain inhibitors. This included PD 150606 that inhibits the proteolytic domain and PD 151746 that inhibits the Ca^{2+} activation domain. Following this step, neutrophils were exposed to 10% cyclic stretch for 3 h (Fig. 5B). Using this approach, we found that pre-treatment with PD 150606 or PD 151746 leads to 4.16 ± 1.60-fold ($P < 0.0001$) and 3.7 ± 1.6-fold ($P < 0.0001$) decrease in the percentage of neutrophils with decondensed nuclei, compared to the vehicle control group (Fig. 5C). Furthermore, pre-treatment with PD 145305, which is the inactive analogue of PD 150606, did not affect stretch-induced NETosis, confirming that Calpain activity is an important modulator of NETosis in response to cyclic stretch and substrate stiffness.

Discussion

In this study, we report for the first time that cyclic stretch and substrate stiffness increase an important biological function of neutrophils, NETosis, as shown by increased chromatin decondensation and accumulation of CitH3, and improve the sensitivity of neutrophils to NETosis-inducing agents such as LPS, PMA, and ATP.

Vascular aging and consequent increase in arterial stiffness is an independent risk factor for cardiovascular morbidity and mortality [62]. Increased arterial stiffness leads to alterations in blood flow-induced forces, such as cyclic deformation of the vessel wall, which affects the mechanobiology of cells exposed to it including the

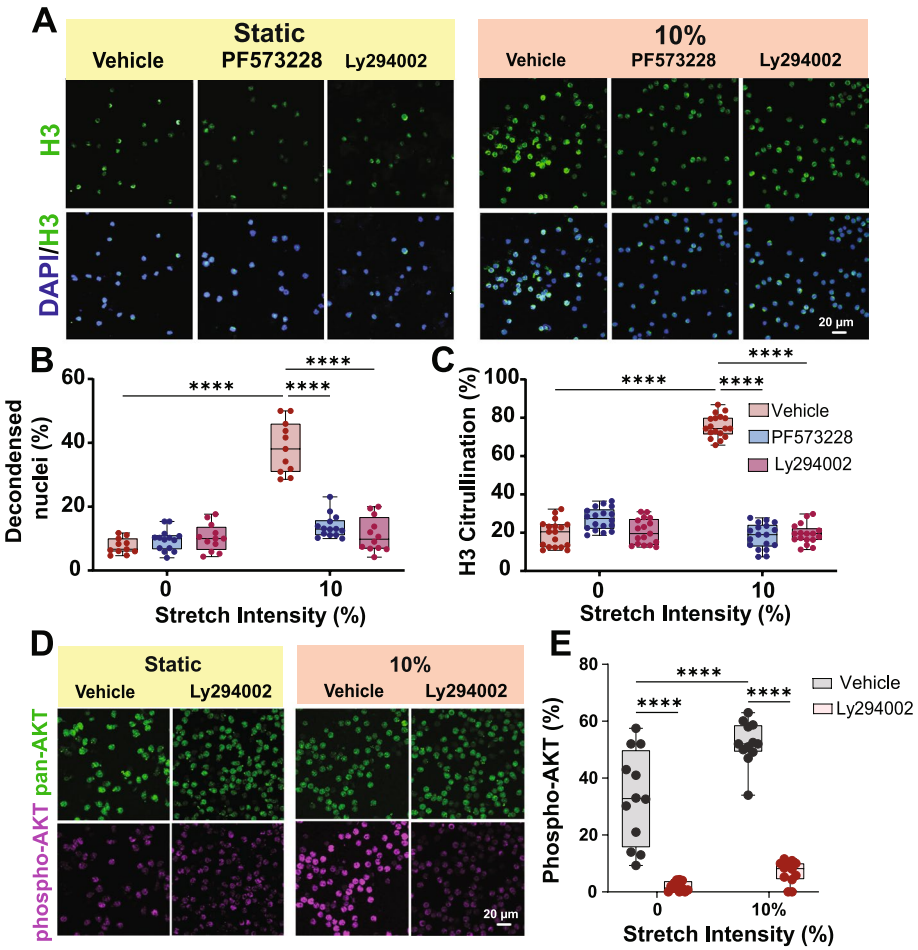

Fig. 3 Contribution of PI3K signaling pathway in neutrophil responses to cyclic stretch and substrate stiffness. **A** Representative immunofluorescence images of human neutrophils pretreated with PF573228 (100 nM) or Ly294002 (10 μM) in the presence or absence of 10% cyclic stretch and substrate stiffness of 300 kPa and stained with DAPI and citrullinated histone H. Bar graphs show **B** normalized percentage of cells with decondensed chromatin, of neutrophils stained with DAPI and **C** normalized percentage of cells stained positive for citrullinated histone after neutrophils pretreated with PF573228 or Ly294002 in the presence of 10% cyclic stretch or static condition and a substrate stiffness of 300 kPa. **D** Representative confocal images of neutrophils pretreated with Ly294002 in the presence of 10% cyclic stretch or static condition and a substrate stiffness of 300 kPa and stained with pan-AKT and phospho-AKT. **E** Representative bar graph showing the percentage of phospho-AKT intensity. Boxes show the median and first and third quartiles. Whiskers represent minimum to maximum values. Bar graphs are representative of at least 3 independent experiments, and each dots represents a randomly selected field of view and at least three images have been analyzed per experiment. Statistical significance was calculated using two-way ANOVA and multiple comparison tests. $^{****}P < 0.0001$

inflammatory cells that are attached to the lumen or have migrated into the subendothelial layer. Neutrophils are polymorphonuclear leukocytes that are very well recognized for their role in host defense but, in addition, play important roles in cardiovascular diseases [63].

NETosis at its early stage is defined by nuclear decondensation and decoration of chromatin with bactericidal proteins from granules and cytoplasm. During NETosis, H3 is deaminated in arginine residues and converted to citrulline (citrullination)- by protein arginine deiminase PAD4 [64]. CitH3 is widely used as a NETosis marker in both in vitro and in vivo studies [58]. In this study, we assessed the effect of cyclic stretch and stiffness, on nuclear decondensation and CitH3 accumulation, as central markers of NETosis. We showed that increase in stretch intensity and substrate stiffness resulted in an increase of the density of neutrophils with decondensed nuclei and CitH3. Furthermore, we observed that exposure of neutrophils to NET-inducing agents is improved in the presence of cyclic stretch in a stretch- and stiffness-dependent manner.

Since the first description of NETs in 2004 [6], many studies have been conducted on NET formation in response to NETs-inducing agents, including pathogens

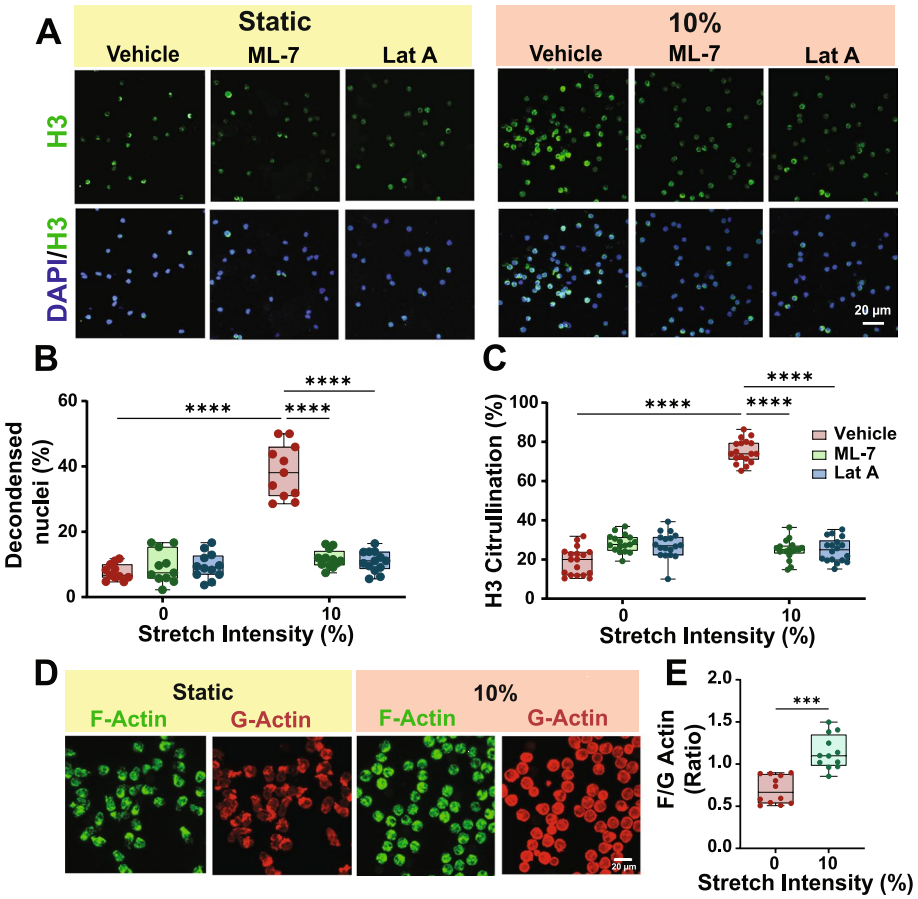

Fig. 4 Contribution of cytoskeleton remodeling in neutrophil responses to cyclic stretch and substrate stiffness. **A** Representative immunofluorescence images of human neutrophils pretreated with ML-7 (10 μM) or latrunculin A (0.02 M), in the presence or absence of 10% cyclic stretch and substrate stiffness of 300 kPa and stained with DAPI and citrullinated histone H. Bar graphs show **B** normalized percentage of cells with decondensed chromatin, of neutrophils stained with DAPI and **C** normalized percentage of cells stained positive for citrullinated histone after neutrophils pretreated with ML-7 or latrunculin A in the presence of 10% cyclic stretch or static condition and a substrate stiffness of 300 kPa. **D** Representative confocal images of neutrophils in the presence of 10% cyclic stretch or static conditions and a substrate stiffness of 300 kPa, stained with Alexa Fluor 488 Deoxyribonuclease I to label G-actin and Atto 565 phalloidin to label F-actin. **E** Representative bar graph showing the ratio of F/G actin. Boxes show the median and first and third quartiles. Whiskers represent minimum to maximum values. Bar graphs are representative of at least 3 independent experiments, and each dots represents a randomly selected field of view and at least 3 images have been analyzed per experiment. Statistical significance was calculated using two-way ANOVA and multiple comparison tests. ***$P < 0.001$ and ****$P < 0.0001$

and bacterial products such as LPS and β-glucan [20, 65–67], physiological stimuli such as ATP, IL-6 or IL-8, platelets, calcium and glucose [66, 68], and substances such as PMA and H_2O_2 [66]. In addition to the above-mentioned stimuli, different environmental factors, such as UV radiation or serum starvation, may also induce NETosis [69–71]. For example, it has been shown that UV radiation can lead to chromatin decondensation, histone citrullination, and NETosis. The addition of fetal calf serum, 0.5% human serum albumin, or 0.5% bovine serum albumin can effectively prevent NET formation in human neutrophils following stimulation with LPS but not after stimulation with PMA or ATP [72, 73]. Thus, serum components inhibit NET formation to varying degrees, depending on the NETosis inducer used. However, the synergistic effects of cyclic stretch on NETs-inducing agents such as PMA, LPS, and ATP is not well understood. To address this gap, in this study, we investigated the effect of cyclic stretch on NETosis, induced by PMA, LPS, and ATP. Our data demonstrate that increase in cyclic stretch intensity significantly improves the sensitivity of neutrophils to all NETs-inducing agents and increases the NET area. In addition, we found that NETosis induced by PMA was reinforced by cyclic stretch, but it was independent of substrate stiffness. However, the stiffness improved NETosis, induced by LPS and ATP. This finding is consistent with previous reports showing that NETosis induced by PMA is completely independent

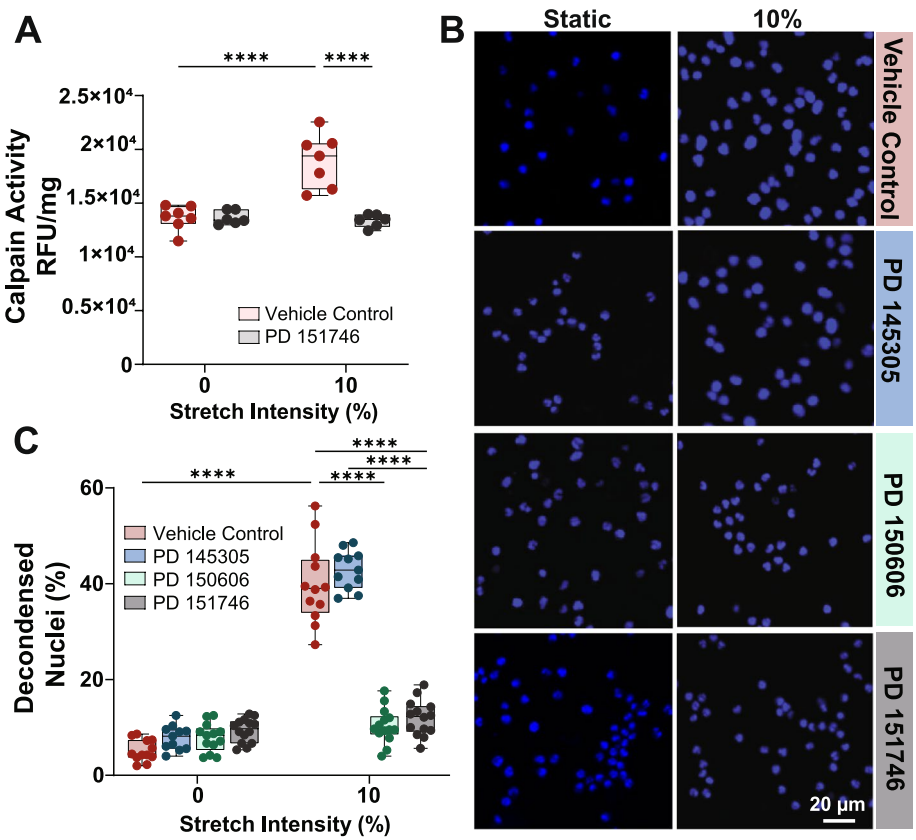

Fig. 5 Calpain activity controls stretch-induced NETosis. **A** Calpain activity assay in neutrophils pretreated with Calpain inhibitor; PD 151746 (20 µM) and vehicle control and exposed to 0–10% cyclic stretch. Bar graph in A represent 3 independent experiments. **B** Representative immunofluorescence images. **C** Percentage of decondensed chromatin in neutrophils pretreated with Calpain inhibitor; PD 150606 (3 µM), PD 151746 (20 µM) and inactive analogue; PD 145305 (20 µM) and vehicle control and exposed to 0–10% cyclic stretch. Boxes show the median and first and third quartiles. Whiskers represent minimum to maximum values. Bar graph in **C** represent at least 3 independent experiments, and each dot represents a randomly selected field of view, and at least 3 images have been analyzed per experiment. Statistical significance was calculated using two-way ANOVA and multiple comparison tests. ****$P < 0.0001$

of adhesion, while NETosis induced by LPS depends on adhesion and substrate elasticity [11]. These data confirms that change in tissue mechanics is potentially directing the role of neutrophils in inflammation.

The rearrangement of the actin cytoskeleton plays a crucial role in various cellular functions, including NETosis triggered by LPS and PMA [74, 75]. Following PMA treatment, neutrophils undergo rapid actin polymerization, reaching peak levels at 60 min before gradually returning to baseline by 180 min [76]. Furthermore, it is shown that neutrophil elastase degrades F-actin within 30 min of exposure to Candida albicans [77]. Here, we found that inhibition of actin polymerization and MLCK activity blocks the effect of cyclic stretch on nuclear decondensation and H3 citrullination. This is most likely due to the lack of translocation of neutrophil elastase to the nucleus, which is also reported in other examples of decreased NETosis [76]. In addition, it is found that cyclic stretch increases the ratio of F to G actin. Overall, our findings here confirmed that cyclic stretch induces cytoskeleton remodeling, which controls NETosis.

The PI3K/AKT signaling pathway is important in transducing hemodynamic forces in endothelial cells and inflammatory blood cells [16, 60]. Here, we showed that both PI3K and FAK activity are important in stretch-induced H3Cit and nuclear decondensation. Furthermore, we found that activation of PI3K is important for AKT activity in response to cyclic stretch. This finding is consistent with previous reports and suggests that neutrophils are using a common mechanosensory pathway to respond to mechanical stretch.

Citrullination of histones during NETosis is regulated via the elevation of intracellular calcium level and Calpain activity [78]. Here, we show that cyclic stretch induces Calpain activity and stretch-induced H3Cit and show that nuclear decondensation can be mitigated by Calpain inhibitors. This is also consistent with previous reports showing that inhibition of Calpain will reduce

the inflammatory response to mechanical ventilation [79]. Confirming these findings, several studies have demonstrated that the calcium ionophores A23187 and ionomycin can induce NETosis [66, 80–84]. Additionally, other studies have shown that treatment of neutrophils with ionophore A23187 leads to rapid deimination of histone H3 and its association with DNA [4] and that A23187 activates NETosis in human polymorphonuclear neutrophils as efficiently as PMA, resulting in NET release [82]. These findings highlight the contribution of intracellular calcium levels upstream of calpain activity in regulating NETosis.

Conclusions

In conclusion, we demonstrate for the first time that cyclic stretch and substrate stiffness induces NETosis and improves the sensitivity of neutrophils to other NETosis inducing agents. Our data also shows that this process is dependent on cytoskeleton remodeling and activation of Calpain, PI3K, and FAK (Fig. 6). These findings provide unique evidence that tissue mechanics contributes to neutrophil-driven inflammatory responses and identify new therapeutic targets.

Methods

Cyclic stretch machine

We used an automated cyclic stretch device, previously developed by our group [33, 85]. The system takes advantage of 3D printed cam and followers for the cyclic deformation of stretchable cell culture wells made of polydimethylsiloxane (PDMS). The device accommodates four stretchable wells, each divided into four compartments, enabling us to perform 16 parallel experiments. The system allowed us to modulate the profile, magnitude, frequency of the cyclic cell stretch, and stiffness of the substrate, as comprehensively discussed in [33, 85].

Preparation of PDMS cell culture chamber with different stiffness

PDMS substrates with different stiffness levels were fabricated using the silicone elastomer kit (DowCorning, Barry, UK) by adding the base and curing agents at weight ratios of 1:45 and 1:25 to achieve the elastic moduli 30 and 300 kPa, respectively. Around 0.05 to 0.07 g of the PDMS mixture was poured on each side well of cell culture chamber and cured at the room temperature for 48 h. The stiffness of the PDMS hydrogels were measured using a rheometer (Discovery HR-3, TA Instruments) and the methodology described before [85]. PDMS wells were then UV-sterilized for 20 min and coated 10 µg/mL with collagen 1 (Cultrex Bovine Collagen I) at 37 °C for 1 h before cell culture to improve neutrophil adhesion.

Human neutrophil isolation

All experiments with human blood were approved by the Ethics Committee of RMIT University (Protocol

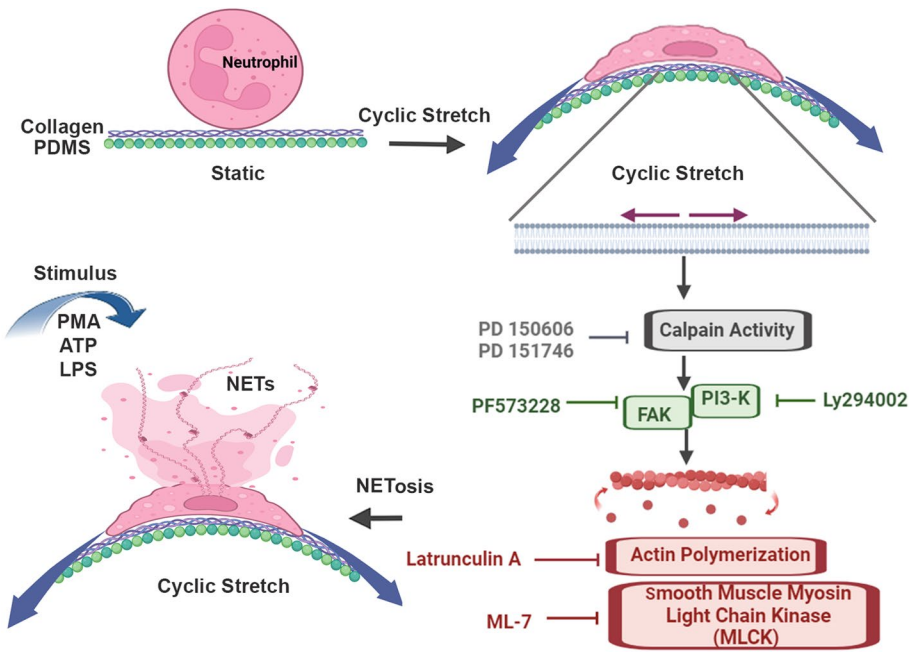

Fig. 6 Schematic diagram showing the effects of cyclic stretch and substrate stiffness on NETosis (figure created with BioRender.com)

Number: 24280), and all donors gave informed voluntary consent.

Peripheral blood (10 mL) was collected from healthy donors in Citrate 3.2% coated vacutainers (S-Monovette® 8.2 mL 9NC). Neutrophils were isolated following standard protocol [11] using a Histopaque double-density gradient created by layering 3 mL of the Histopaque-1077 solution (Sigma-Aldrich) above the Histopaque-1119 solution (Sigma-Aldrich). The purity of neutrophils was assessed using the Sysmex Cell counter (Sysmex, Japan). In all experiments, neutrophil viability and purity were above 98% and 87%, respectively. After isolation, neutrophils were rested in the incubator for 45 min at 37 °C and 5% CO_2 before exposure to cyclic stretch.

Neutrophil culture on elastomeric wells

Cyclic stretch stimulation of cells was performed using protocols previously described [33]. In short, after coating PDMS chambers with collagen 1, extracellular matrix solutions were aspirated, and neutrophils were then plated at the density of 300,000 cells/well and incubated for 20 min to allow them to adhere.

For cyclic stretch experiments, neutrophils were cultured inside the PDMS chambers and were allowed to adhere for 20 min. Next, chambers were loaded onto the device and subjected to 5% or 10% cyclic stretch at 1 Hz for 3 h at 37 °C and 5% CO_2. Static condition wells were just left in the incubator for the same timeframe.

For drug stimulation, neutrophils were treated with 75 nM phorbol 12-myristate 13-acetate (PMA) (Merck, Australia), 100 nM adenosine triphosphate (ATP) (Sigma, USA) prepared with competed RPMI-1640 complete medium, or 10 µg/mL lipopolysaccharides (LPS) from *Escherichia coli* (Sigma, Australia) prepared with serum-free RPMI-1640 medium, to induce the release of NETs in the presence or absence of cyclic stretch. Here, we assessed the effect of LPS in serum-free media, as previous reports have demonstrated that the addition of fetal calf serum effectively inhibits NETosis in response to LPS [72, 73]. To identify the downstream signaling pathway activated post cyclic stretch stimulation, isolated neutrophils were pre-incubated for 45 min in 5% CO_2 at 37 °C with mechanotransduction pathway inhibitors such as 10 µM Ly294002 (PI3K inhibitors), 100 nM PF573228 (FAK inhibitor), 0.02 M latrunculin A (Actin Polymerization inhibitor), 10 µM ML-7-Hydrochloride (Myosin Light Chain Kinase (MLCK) inhibitor), 20 µM PD 145305 (Negative control for the calpain inhibitors, 3 µM PD 150606 (Uncompetitive calpain inhibitor), and 20 µM PD 151746 (Cell-permeable calpain inhibitor).

Immunofluorescence staining

For immune staining, cells were fixed with 4% paraformaldehyde (PFA) for 30 min at 37 °C. Neutrophils were permeabilized with 0.1% Triton X-100 for 15 min and blocked with 4% goat serum for 30 min at 37 °C to remove non-specific antibody binding. Next, samples were stained with 5 µg/mL rabbit anti-histone H3 (citrulline R2 + R8 + R17, #ab5103) from Abcam, Australia, overnight at 4 °C. The secondary antibody staining was achieved using AF647 goat anti-rabbit IgG or AF488 goat anti-rabbit IgG (Invitrogen, Australia). The isotype control, Rabbit IgG (Vector Laboratories), was used for this staining to differentiate genuine target staining from background (Supplementary Fig. 2).

DNA staining to NETosis was performed using 2 µg/mL DAPI for 5 min. The AKT activity was assessed by staining neutrophils post-fixation with pan-AKT mouse monoclonal antibody (2920, Cell Signaling) to label total AKT and phospho-AKT (Ser473) rabbit monoclonal antibody (4060, Cell Signaling) to label phosphorylated AKT. Alexa Fluor 488-conjugated goat anti-mouse IgG and Alexa Fluor 647-conjugated goat anti-rabbit IgG (both from Invitrogen, Australia) were used as secondary antibodies. For this assay, all staining and washing steps were performed using Tris-buffered saline (pH 7.2). To assess actin dynamics, neutrophils were fixed with 4% paraformaldehyde for 1 h at 37 °C, permeabilized with 0.1% Triton X-100 in PBS for 10 min, and then stained with Alexa Fluor 488-conjugated Deoxyribonuclease I (D12371, Invitrogen, Australia) to label G-actin and Atto 565-conjugated phalloidin (#94,072, Sigma Australia) to label F-actin.

Confocal imaging and image analysis

All image acquisitions were obtained with a Nikon A1MP Multiphoton microscope controlled by Nikon Elements software (Nikon, Japan) with a 20× objective lens and 4× camera zoom. Six random fields of view were selected, and Z-series optical sections with a step size of 0.5 µm were acquired. All images from the same experiment were obtained using the same device settings. All images were photographed using a resolution of 512 × 512 pixels with a scan speed of 4.8 pixels dwell time and scanned sequentially to reduce fluorescence bleed-through.

Image processing of NETs production was performed using a custom macro and ImageJ software (Supplementary Fig. 3). Briefly, confocal images of DNA staining using DAPI were thresholded to include NETs while excluding intact nuclei, and the area covered by NETs was quantified and normalized to the number of cells. The percentage of decondensed nuclei was calculated by counting the number of circulated neutrophils present in

the field of view against the total number of cells using NIS element software.

Calpain activity assay

The Calpain Activity Assay Kit (Abcam, Cambridge, MA, USA, #ab65308) was used to quantify relative Calpain enzyme activity following suppliers' instructions. After each experiment, neutrophils were suspended in extraction buffer and then samples were centrifuged at 21,000 × g for 10 min at 4 °C. Supernatants were transferred to a fresh, ice-cold tube, and protein content was quantified using a Pierce BCA Protein Assay (Thermo Fisher Scientific, Waltham, MA, USA). Next, Calpain activity changes in relative fluorescent units were detected using a CLARIOStar-BMG-Plate Reader. As control, isolated neutrophils were treated with PD 151746; cell-permeable Calpain inhibitor, providing a negative control for the assay, and active Calpain was examined as a positive control.

Statistics and data analysis

Statistics were done with GraphPad Prism (Version 9.0, GraphPad Software Inc., San Diego, California). All data are presented as mean ± standard deviation (SD). Boxes on all figures show the median and first and third quartiles on the figures. Whiskers represent minimum to maximum values and show all points. Significance was tested using standard two-way ANOVA with multiple comparisons test ($^{*}P<0.05$, $^{**}P<0.01$, $^{***}P<0.001$ and $^{****}P<0.0001$).

Abbreviations

NETs	Neutrophils extracellular traps
CitH3	Citrullination of histone H3
PMA	Phorbol 12-myristate 13-acetate
ATP	Adenosine triphosphate
LPS	Lipopolysaccharides
PI3K	Phosphatidylinositol 3-kinase
FAK	Focal adhesion kinase
CVDs	Cardiovascular diseases
PDMS	Polydimethylsiloxane
MLCK	Myosin light chain kinase
PFA	Paraformaldehyde
SD	Standard deviation

Supplementary Information

The online version contains supplementary material available at https://doi.org/10.1186/s12915-024-02009-6.

Additional file 1: Supplementary Fig. 1. PMA, LPS, and ATP-induced NETosis under static conditions. Bar graphs show NET areas normalized to total cell number in the presence of Vehicle control, PMA (75 nM), LPS (10 µg/mL), or ATP (100 nM) on substrates with stiffnesses of 30 kPa and 300 kPa. Boxes represent the median and first and third quartiles. Whiskers represent minimum to maximum values. The bar graphs are representative of at least four independent experiments, with each dot representing a randomly selected field of view, and at least three images per experiment. Statistical significance was calculated using two-way ANOVA and multiple comparison tests. $^{*}P<0.05$, $^{**}P<0.01$, $^{***}P<0.001$, and $^{****}P<0.0001$. Supplementary Fig. 2. Isotype control confirming the specificity of anti-rabbit H3. Representative immunofluorescence images of human neutrophils stained with Rabbit IgG as an isotype control, followed by DAPI and (A) Alexa 647 goat anti-rabbit or (B) Alexa 488 goat anti-rabbit. Supplementary Fig. 3. NET area analysis. The confocal image (Step 1) is utilized to generate the intensity profile image using ImageJ (Step 2). In the confocal image (Step 1), the bright blue objects highlighted by red arrows represent the nucleus, while the light blue objects highlighted by white arrows indicate NETs. Using the intensity profile image in Step 2, areas not covered by NETs and nucleus structures are excluded from the analysis, and only the total NET area is selected and measured, as depicted by the black colour in Step 3.

Acknowledgements

The authors are most grateful to the blood donors for their collaboration. They thank Dr. Adam Parslow, for his excellent technical support in confocal microscope imaging.

Authors' contributions

MK conducted experiments, analyzed the results, and wrote the manuscript. CC, HD, NCS and SA performed experiments and wrote the manuscript. KP and KK analyzed the results, and wrote the manuscript. SB led the work, designed experiments, analyzed the results, and wrote the manuscript.

Funding

This work was supported by the National Health and Medical Research Council (NHMRC) for Ideas grant (No. 2020197) to S.B, K.K and K.P and a L3 Investigator Fellowship support (GNT1174098) to K.P, the Australian Research Council for Discovery grant (No. DP200101248) to S.B and K.K, and the Australian Government Research Training Program Scholarship to M.K.

Availability of data and materials

All data supporting the findings of this study are included within the published work.
Link to the custom macro used to analyzed NET area can be accessed via this link: https://figshare.com/s/20cca5a03cf4a90e8dce. All future communication should be directed to the corresponding author.

Declarations

Ethics approval and consent to participate

All experiments with human blood were approved by the Ethics Committee of RMIT University (Protocol Number: 24280), and all donors gave informed voluntary consent.

Consent for publication

Not applicable.

Competing interests

The authors declare no competing interests.

Received: 24 May 2024 Accepted: 5 September 2024
Published online: 18 September 2024

References

1. Yan J, Kloecker G, Fleming C, Bousamra M 2nd, Hansen R, Hu X, et al. Human polymorphonuclear neutrophils specifically recognize and kill cancerous cells. Oncoimmunology. 2014;3(7):e950163.
2. Kaplan MJ, Radic M. Neutrophil extracellular traps: double-edged swords of innate immunity. J Immunol. 2012;189(6):2689–95.
3. Wang J. Neutrophils in tissue injury and repair. Cell Tissue Res. 2018;371(3):531–9.
4. Butterfield TA, Best TM, Merrick MA. The dual roles of neutrophils and macrophages in inflammation: a critical balance between tissue damage and repair. J Athl Train. 2006;41(4):457.

5. Clancy DM, Henry CM, Sullivan GP, Martin SJ. Neutrophil extracellular traps can serve as platforms for processing and activation of IL-1 family cytokines. The FEBS J. 2017;284(11):1712–25.
6. Brinkmann V, Reichard U, Goosmann C, Fauler B, Uhlemann Y, Weiss DS, et al. Neutrophil extracellular traps kill bacteria. Science. 2004;303(5663):1532–5.
7. Fuchs TA, Abed U, Goosmann C, Hurwitz R, Schulze I, Wahn V, et al. Novel cell death program leads to neutrophil extracellular traps. J Cell Biol. 2007;176(2):231–41.
8. Lood C, Blanco LP, Purmalek MM, Carmona-Rivera C, De Ravin SS, Smith CK, et al. Neutrophil extracellular traps enriched in oxidized mitochondrial DNA are interferogenic and contribute to lupus-like disease. Nat Med. 2016;22(2):146–53.
9. Neubert E, Meyer D, Rocca F, Günay G, Kwaczala-Tessmann A, Grandke J, et al. Chromatin swelling drives neutrophil extracellular trap release. Nat Commun. 2018;9(1):1–13.
10. Gimbrone MA Jr, García-Cardeña G. Endothelial cell dysfunction and the pathobiology of atherosclerosis. Circ Res. 2016;118(4):620–36.
11. Erpenbeck L, Gruhn AL, Kudryasheva G, Günay G, Meyer D, Busse J, et al. Effect of adhesion and substrate elasticity on neutrophil extracellular trap formation. Front Immunol. 2019;10: 2320.
12. Urban CF, Reichard U, Brinkmann V, Zychlinsky A. Neutrophil extracellular traps capture and kill Candida albicans yeast and hyphal forms. Cell Microbiol. 2006;8(4):668–76.
13. Saitoh T, Komano J, Saitoh Y, Misawa T, Takahama M, Kozaki T, et al. Neutrophil extracellular traps mediate a host defense response to human immunodeficiency virus-1. Cell Host Microbe. 2012;12(1):109–16.
14. Martinod K, Wagner DD. Thrombosis: tangled up in NETs. Blood. 2014;123(18):2768–76.
15. Yu X, Tan J, Diamond SL. Hemodynamic force triggers rapid NETosis within sterile thrombotic occlusions. J Thromb Haemost. 2018;16(2):316–29.
16. Abaricia JO, Shah AH, Olivares-Navarrete R. Substrate stiffness induces neutrophil extracellular trap (NET) formation through focal adhesion kinase activation. Biomaterials. 2021;271:120715.
17. Laurent S, Boutouyrie P. The structural factor of hypertension: large and small artery alterations. Circ Res. 2015;116(6):1007–21.
18. Birukov KG, Bardy N, Lehoux S, Merval R, Shirinsky VP, Tedgui A. Intraluminal pressure is essential for the maintenance of smooth muscle caldesmon and filamin content in aortic organ culture. Arterioscler Thromb Vasc Biol. 1998;18(6):922–7.
19. Birukov KG. Cyclic stretch, reactive oxygen species, and vascular remodeling. Antioxid Redox Signal. 2009;11(7):1651–67.
20. Bardy N, Merval R, Benessiano J, Samuel JL, Tedgui A. Pressure and angiotensin II synergistically induce aortic fibronectin expression in organ culture model of rabbit aorta. Evidence for a pressure-induced tissue renin-angiotensin system. Circ Res. 1996;79(1):70–8.
21. Kakisis JD, Liapis CD, Sumpio BE. Effects of cyclic strain on vascular cells. Endothelium. 2004;11(1):17–28.
22. Ando J, Yamamoto K. Vascular mechanobiology: endothelial cell responses to fluid shear stress. Circ J. 2009;73(11):1983–92.
23. Hipper A, Isenberg G. Cyclic mechanical strain decreases the DNA synthesis of vascular smooth muscle cells. Pflugers Arch. 2000;440(1):19–27.
24. Leloup A, De Moudt S, Van Hove C, Fransen P. Cyclic stretch alters vascular reactivity of mouse aortic segments. Front Physiol. 2017;8: 858.
25. Anwar MA, Shalhoub J, Lim CS, Gohel MS, Davies AH. The effect of pressure-induced mechanical stretch on vascular wall differential gene expression. J Vasc Res. 2012;49(6):463–78.
26. Jufri NF, Mohamedali A, Avolio A, Baker MS. Mechanical stretch: physiological and pathological implications for human vascular endothelial cells. Vasc Cell. 2015;7:8.
27. Mann JM, Lam RH, Weng S, Sun Y, Fu J. A silicone-based stretchable micropost array membrane for monitoring live-cell subcellular cytoskeletal response. Lab Chip. 2012;12(4):731–40.
28. Yan J, Wang WB, Fan YJ, Bao H, Li N, Yao QP, et al. Cyclic stretch induces vascular smooth muscle cells to secrete connective tissue growth factor and promote endothelial progenitor cell differentiation and angiogenesis. Front Cell Dev Biol. 2020;8: 606989.
29. Liu B, Qu MJ, Qin KR, Li H, Li ZK, Shen BR, et al. Role of cyclic strain frequency in regulating the alignment of vascular smooth muscle cells in vitro. Biophys J. 2008;94(4):1497–507.
30. Kamble H, Vadivelu R, Barton M, Boriachek K, Munaz A, Park S, et al. An electromagnetically actuated double-sided cell-stretching device for mechanobiology research. Micromachines (Basel). 2017;8(8):256.
31. Kamble H, Vadivelu R, Barton M, Shiddiky MJA, Nguyen NT. Pneumatically actuated cell-stretching array platform for engineering cell patterns in vitro. Lab Chip. 2018;18(5):765–74.
32. Estrada R, Giridharan GA, Nguyen MD, Roussel TJ, Shakeri M, Parichehreh V, et al. Endothelial cell culture model for replication of physiological profiles of pressure, flow, stretch, and shear stress in vitro. Anal Chem. 2011;83(8):3170–7.
33. Aguilera Suarez S, Sekar NC, Nguyen N, Lai A, Thurgood P, Zhou Y, et al. Studying the mechanobiology of aortic endothelial cells under cyclic stretch using a modular 3D printed system. Front Bioeng Biotechnol. 2021;9: 791116.
34. Dharmashankar K, Widlansky ME. Vascular endothelial function and hypertension: insights and directions. Curr Hypertens Rep. 2010;12(6):448–55.
35. Wolinsky H, Glagov S. Comparison of abdominal and thoracic aortic medial structure in mammals. Deviation of man from the usual pattern. Circ Res. 1969;25(6):677–86.
36. Wolinsky H, Glagov S. Structural basis for the static mechanical properties of the aortic media. Circ Res. 1964;14:400–13.
37. Zieman SJ, Melenovsky V, Kass DA. Mechanisms, pathophysiology, and therapy of arterial stiffness. Arterioscler Thromb Vasc Biol. 2005;25(5):932–43.
38. Martinod K, Witsch T, Erpenbeck L, Savchenko A, Hayashi H, Cherpokova D, et al. Peptidylarginine deiminase 4 promotes age-related organ fibrosis. J Exp Med. 2017;214(2):439–58.
39. Lelliott PM, Momota M, Lee MSJ, Kuroda E, Iijima N, Ishii KJ, et al. Rapid quantification of NETs in vitro and in whole blood samples by imaging flow cytometry. Cytometry A. 2019;95(5):565–78.
40. Leshner M, Wang S, Lewis C, Zheng H, Chen XA, Santy L, et al. PAD4 mediated histone hypercitrullination induces heterochromatin decondensation and chromatin unfolding to form neutrophil extracellular trap-like structures. Front Immunol. 2012;3:307.
41. Costantino S, Paneni F, Cosentino F. Ageing, metabolism and cardiovascular disease. J Physiol. 2016;594(8):2061–73.
42. Mitchell GF, Hwang SJ, Vasan RS, Larson MG, Pencina MJ, Hamburg NM, et al. Arterial stiffness and cardiovascular events: the Framingham Heart Study. Circulation. 2010;121(4):505–11.
43. Adlerz KM, Aranda-Espinoza H, Hayenga HN. Substrate elasticity regulates the behavior of human monocyte-derived macrophages. Eur Biophys J. 2016;45(4):301–9.
44. Blakney AK, Swartzlander MD, Bryant SJ. The effects of substrate stiffness on the in vitro activation of macrophages and in vivo host response to poly(ethylene glycol)-based hydrogels. J Biomed Mater Res A. 2012;100(6):1375–86.
45. Mennens SFB, Bolomini-Vittori M, Weiden J, Joosten B, Cambi A, van den Dries K. Substrate stiffness influences phenotype and function of human antigen-presenting dendritic cells. Sci Rep. 2017;7(1):17511.
46. Matsumoto T, Abe H, Ohashi T, Kato Y, Sato M. Local elastic modulus of atherosclerotic lesions of rabbit thoracic aortas measured by pipette aspiration method. Physiol Meas. 2002;23(4):635–48.
47. Georges PC, Hui JJ, Gombos Z, McCormick ME, Wang AY, Uemura M, et al. Increased stiffness of the rat liver precedes matrix deposition: implications for fibrosis. Am J Physiol Gastrointest Liver Physiol. 2007;293(6):G1147–54.
48. Denis M, Gregory A, Bayat M, Fazzio RT, Whaley DH, Ghosh K, et al. Correlating tumor stiffness with immunohistochemical subtypes of breast cancers: prognostic value of comb-push ultrasound shear elastography for differentiating luminal subtypes. PLoS One. 2016;11(10): e0165003.
49. Jannat RA, Robbins GP, Ricart BG, Dembo M, Hammer DA. Neutrophil adhesion and chemotaxis depend on substrate mechanics. J Phys Condens Matter. 2010;22(19): 194117.
50. Oakes PW, Patel DC, Morin NA, Zitterbart DP, Fabry B, Reichner JS, et al. Neutrophil morphology and migration are affected by substrate elasticity. Blood. 2009;114(7):1387–95.
51. Stroka KM, Aranda-Espinoza H. Neutrophils display biphasic relationship between migration and substrate stiffness. Cell Motil Cytoskeleton. 2009;66(6):328–41.

52. McDonald B, Urrutia R, Yipp BG, Jenne CN, Kubes P. Intravascular neutrophil extracellular traps capture bacteria from the bloodstream during sepsis. Cell Host Microbe. 2012;12(3):324–33.
53. Morikis VA, Simon SI. Neutrophil mechanosignaling promotes integrin engagement with endothelial cells and motility within inflamed vessels. Front Immunol. 2018;9: 2774.
54. Stroka KM, Aranda-Espinoza H. Endothelial cell substrate stiffness influences neutrophil transmigration via myosin light chain kinase-dependent cell contraction. Blood. 2011;118(6):1632–40.
55. Mohanty T, Sjögren J, Kahn F, Abu-Humaidan AH, Fisker N, Assing K, et al. A novel mechanism for NETosis provides antimicrobial defense at the oral mucosa. Blood. 2015;126(18):2128–37.
56. Rossaint J, Herter JM, Van Aken H, Napirei M, Döring Y, Weber C, et al. Synchronized integrin engagement and chemokine activation is crucial in neutrophil extracellular trap-mediated sterile inflammation. Blood. 2014;123(16):2573–84.
57. Vriz O, Magne J, Driussi C, Brosolo G, Ferrara F, Palatini P, et al. Comparison of arterial stiffness/compliance in the ascending aorta and common carotid artery in healthy subjects and its impact on left ventricular structure and function. Int J Cardiovasc Imaging. 2017;33(4):521–31.
58. Tilley DO, Abuabed U, Zimny Arndt U, Schmid M, Florian S, Jungblut PR, et al. Histone H3 clipping is a novel signature of human neutrophil extracellular traps. eLife. 2022;11:e68283.
59. Remijsen Q, Vanden Berghe T, Wirawan E, Asselbergh B, Parthoens E, De Rycke R, et al. Neutrophil extracellular trap cell death requires both autophagy and superoxide generation. Cell Res. 2011;21(2):290–304.
60. DeSouza-Vieira T, Guimarães-Costa A, Rochael NC, Lira MN, Nascimento MT, Lima-Gomez PdS, et al. Neutrophil extracellular traps release induced by Leishmania: role of PI3Kγ, ERK, PI3Kσ, PKC, and [Ca2+]. J Leukoc Biol. 2016;100(4):801–10.
61. Dewitt S, Francis RJ, Hallett MB. Ca^{2+} and calpain control membrane expansion during the rapid cell spreading of neutrophils. J Cell Sci. 2013;126(Pt 20):4627–35.
62. Cecelja M, Chowienczyk P. Dissociation of aortic pulse wave velocity with risk factors for cardiovascular disease other than hypertension. Hypertension. 2009;54(6):1328–36.
63. Döring Y, Libby P, Soehnlein O. Neutrophil extracellular traps participate in cardiovascular diseases: recent experimental and clinical insights. Circ Res. 2020;126(9):1228–41.
64. Wang Y, Li M, Stadler S, Correll S, Li P, Wang D, et al. Histone hypercitrullination mediates chromatin decondensation and neutrophil extracellular trap formation. J Cell Biol. 2009;184(2):205–13.
65. Delgado-Rizo V, Martínez-Guzmán MA, Iñiguez-Gutierrez L, García-Orozco A, Alvarado-Navarro A, Fafutis-Morris M. Neutrophil extracellular traps and its implications in inflammation: an overview. Front Immunol. 2017;8:81.
66. Hoppenbrouwers T, Autar ASA, Sultan AR, Abraham TE, van Cappellen WA, Houtsmuller AB, et al. In vitro induction of NETosis: comprehensive live imaging comparison and systematic review. PLoS One. 2017;12(5):e0176472.
67. Pieterse E, Rother N, Yanginlar C, Hilbrands LB, van der Vlag J. Neutrophils discriminate between lipopolysaccharides of different bacterial sources and selectively release neutrophil extracellular traps. Front Immunol. 2016;7:484.
68. Vorobjeva NV, Chernyak BV. NETosis: molecular mechanisms, role in physiology and pathology. Biochemistry (Mosc). 2020;85(10):1178–90.
69. Neubert E, Bach KM, Busse J, Bogeski I, Schön MP, Kruss S, et al. Blue and long-wave ultraviolet light induce in vitro neutrophil extracellular trap (NET) formation. Front Immunol. 2019;10: 2428.
70. Arzumanyan G, Mamatkulov K, Arynbek Y, Zakrytnaya D, Jevremović A, Vorobjeva N. Radiation from UV-A to red light induces ROS-dependent release of neutrophil extracellular traps. Int J Mol Sci. 2023;24(6):5770.
71. Azzouz D, Palaniyar N. Mitochondrial ROS and base excision repair steps leading to DNA nick formation drive ultraviolet induced-NETosis. Front Immunol. 2023;14: 1198716.
72. Neubert E, Senger-Sander SN, Manzke VS, Busse J, Polo E, Scheidmann SEF, et al. Serum and serum albumin inhibit in vitro formation of neutrophil extracellular traps (NETs). Front Immunol. 2019;10: 12.
73. Kamoshida G, Kikuchi-Ueda T, Nishida S, Tansho-Nagakawa S, Kikuchi H, Ubagai T, et al. Spontaneous formation of neutrophil extracellular traps in serum-free culture conditions. FEBS Open Bio. 2017;7(6):877–86.
74. Neeli I, Dwivedi N, Khan S, Radic M. Regulation of extracellular chromatin release from neutrophils. J Innate Immun. 2009;1(3):194–201.
75. Sprenkeler EGG, Tool ATJ, Henriet SSV, van Bruggen R, Kuijpers TW. Formation of neutrophil extracellular traps requires actin cytoskeleton rearrangements. Blood. 2022;139(21):3166–80.
76. Thiam HR, Wong SL, Qiu R, Kittisopikul M, Vahabikashi A, Goldman AE, et al. NETosis proceeds by cytoskeleton and endomembrane disassembly and PAD4-mediated chromatin decondensation and nuclear envelope rupture. Proc Natl Acad Sci U S A. 2020;117(13):7326–37.
77. Metzler KD, Goosmann C, Lubojemska A, Zychlinsky A, Papayannopoulos V. A myeloperoxidase-containing complex regulates neutrophil elastase release and actin dynamics during NETosis. Cell Rep. 2014;8(3):883–96.
78. Gößwein S, Lindemann A, Mahajan A, Maueröder C, Martini E, Patankar J, et al. Citrullination licenses calpain to decondense nuclei in neutrophil extracellular trap formation. Front Immunol. 2019;10:2481.
79. Liu D, Yan Z, Minshall RD, Schwartz DE, Chen Y, Hu G. Activation of calpains mediates early lung neutrophilic inflammation in ventilator-induced lung injury. Am J Physiol Lung Cell Mol Physiol. 2012;302(4):L370–9.
80. Wong SL, Demers M, Martinod K, Gallant M, Wang Y, Goldfine AB, et al. Diabetes primes neutrophils to undergo NETosis, which impairs wound healing. Nat Med. 2015;21(7):815–9.
81. Kenny EF, Herzig A, Krüger R, Muth A, Mondal S, Thompson PR, et al. Diverse stimuli engage different neutrophil extracellular trap pathways. Elife. 2017;6:6.
82. Neeli I, Khan SN, Radic M. Histone deimination as a response to inflammatory stimuli in neutrophils. J Immunol. 2008;180(3):1895–902.
83. Fadini GP, Menegazzo L, Rigato M, Scattolini V, Poncina N, Bruttocao A, et al. NETosis delays diabetic wound healing in mice and humans. Diabetes. 2016;65(4):1061–71.
84. Barrientos L, Marin-Esteban V, de Chaisemartin L, Le-Moal VL, Sandré C, Bianchini E, et al. An improved strategy to recover large fragments of functional human neutrophil extracellular traps. Front Immunol. 2013;4:166.
85. Chandra Sekar N, Aguilera Suarez S, Nguyen N, Lai A, Thurgood P, Zhou Y, et al. Studying the synergistic effect of substrate stiffness and cyclic stretch level on endothelial cells using an elastomeric cell culture chamber. ACS Appl Mater Interfaces. 2023;15(4):4863–72.

Publisher's Note